Journal of Hydroscience and Hydraulic Engineering
Vol. 9, No. 2, January, 1992, 37-45

COMPARISON OF TURBULENCE STRUCTURES BETWEEN AN OPEN CHANNEL FLOW AND A CLOSED DUCT FLOW

By

Yoshihiro ISHII

Graduate Student, Department of Civil Engineering
Tohoku University, Aoba, Sendai 980, Japan

and

Masaki SAWAMOTO

Professor, Department of Civil Engineering
Tohoku University, Aoba, Sendai 980, Japan

SYNOPSIS

Two types of turbulence, an uniform flow and a wake flow behind a vertical cylinder, were measured in an open channel and a closed duct in order to study the dynamical effect of the free surface. Visualization technique was also utilized to observe the organized structure of turbulence. Applicability of the k-ε model was examined. Followings were concluded: 1) A conventional symmetrical boundary condition is inapplicable at the free surface of the open channel. 2) The wake in the open channel is decayed at the shorter distance and the structure of the wall turbulence in the open channel is quickly recovered.

1. INTRODUCTION

Open channel flow is characterized by the existence of the free surface. The boundary conditions at the free surface may be given as the dynamic conditions of the shear free and of the constant pressure. In the case of the uniform flow, the former condition is formulated macroscopically by zero value of velocity gradient at the free surface and the latter is satisfied implicitly through the uniformity of flow. Those facts conclude that open channel flow with the uniform depth h is dynamically equivalent to closed duct flow with thickness 2h and that the condition of the symmetry flow structure at the center line in closed duct flow is a dynamical counterpart at the free surface in open channel flow.

This simplified boundary condition, however, can not be apply directly to the free surface when we discuss the flow structure in detail near the free surface. Especially, the turbulent structure near the free surface can not be guessed from the analogy of that near the center line of the closed duct flow. This is because that the dynamical free surface condition must be satisfied not macroscopically but in every moment. This fact allows the existence as surface gravity waves. The large structure of turbulence like the organized structure of turbulence near the free surface would not be reflected at the free surface so that the symmetrical boundary condition should be satisfied but transfers a part of its energy to the surface wave when it reaches at the free surface. Some researchers (1) tried to explain this by

introducing a coefficient of decay constant in the turbulence model but its mechanism is rather complicated.

The aim of this paper is to investigate the dynamical effect at the free surface experimentally. The turbulent structure in open channel flow is compared with that in closed duct flow in order to study the difference between the free surface and the symmetry line of closed duct flow. Two types of turbulence, was the turbulence of uniform flow and the other is wake flow behind the vertical circular cylinder placed in the uniform flow, were measured. The applicability of the k-ε model is also discussed for uniform flow.

2. EXPERIMENTAL APPARATUS AND PROCEDURES

2.1 Hydraulic conditions

A series of experiments were carried out by using a circulating water flume with the rectangular cross section which enable us to make both open channel flow and closed duct flow. The flume used for these experiments was 10.0m length, 0.36m width and 0.06m depth with 1/200 slope (Figure 1). The side walls and the bottom were of transparent acrylic plates. Water was straightenned by a run-up area, which was made by straightenning vanes and honeycomb filters. Depth was adjusted by the moving gate at downstream in the case of open channel flow. The measuring section was located 5.0m from the upper end and the center of the span. Measurements were carried out in two types of the turbulence of same Reynolds number. One was uniform flow, and the other was in wake of a vertical cylinder(Φ=3.2mm) placed at 45cm up from the measuring point. The coordinate was defined that x axis was longitudinal, y axis was vertical, and z axis was span.

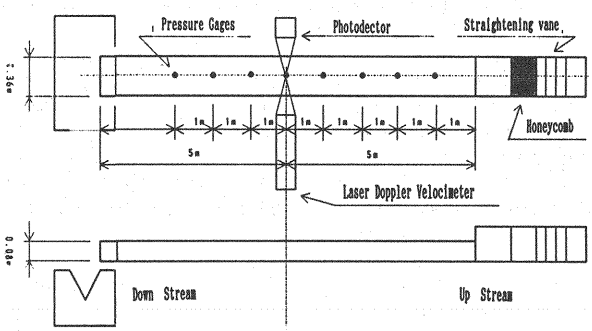

Figure 1 Laboratory flume

Table 1 shows hydraulic conditions of present experiments, ho is the depth in the case of open channel flow and is the half of depth in the case of duct flow.

Table 1 Hydraulic Conditions

Case	Status	ho (cm)	R (cm)	Umax (cm/s)	Uo (cm/s)	U* (cm/s)	Re x10^4	Fr
1	Open/Uniform	2.15	1.92	81.38	69.56	3.63	5.3	1.52
2	Duct/Uniform	3.00	2.57	75.34	75.34	3.72	5.4	1.61
3	Open/Wake	2.00	1.80	57.15	57.15	3.51	5.9	1.36
4	Duct/Wake	3.00	2.57	62.60	62.20	3.72	6.4	1.24

$$Uo=\frac{1}{ho}\int_0^{ho} Udy \quad , \quad Re=\frac{4UoR}{\nu} \quad , \quad Fr=\frac{Uo}{\sqrt{gR}}$$

R:Hydraulic radius

2.2 Velocity measurement

The velocity was measured by a two component type Laser

Doppler Velocimeter (Argon gas laser:λ=632.8nm, 15mW max power) of the forward scattering system. A laser beam was polarized into two components, one is horizontal and the other is vertical. Each beam was splitted into two parallel beams, and one of parallel beams was shifted in frequency. The receiving optics was so set up that is opposite to the transmitting optics and right to the water flume.

Burst signals from a photodetector were transformed to digital data by the analog digital converter. A lock-detector signal was measured together with the burst signal. Those data were recorded onto the flexible disk. The horizontal and vertical data were independently measured. Each component data was checked by the lock-detector signal, and some averaged values were calculated with the only checked one. The number of averages was over 6000 and sampling interval was 0.01 sec. This process carried out by a personal computer (NEC:PC-9801 series).

2.3 Visualization technique

The fluorescent dye injection method was used in order to visualize the large organized structure of turbulence in outer region. Solutions of Methylene Blue and Sudan III were used as the tracer. They were injected with a constant velocity into open channel flow through a small pore drilled on the bottom, and on the upper and lower wall in the the case of closed duct flow. The pores were located at the center of the span and 45cm up the measuring point. The results of the observation were recorded by the 35mm still camera and the 1/2" VTR camera. The VTR images were analyzed through a visual management system (Tohoku Univ.: Image System for On-line Processing).

3. VISUALIZATION

3.1 Open channel flow

Plates 1 to 4 show a series of pictures, recorded by VTR camera and processed by ISOP (Image System for On-line Processing : Tohoku Univ.), with the time interval 1/30sec. Hydraulic condition is CASE 1 in Table 1. The wide black arrow, at the left side of each plates, represents the flow direction. The white part is the tracer and the narrow black arrow indicates the position of the organized structure of turbulence occurred.

The organized structure of turbulence occurs and the tracer begins to lift at the right side (Plate 1). The organized structure of turbulence reaches to the free surface (Plate 2). Tracer is restrained by the only free surface and the organized structure of turbulence flows away (Plate 3). The organized structure of turbulence breaks up and disperses into the surrounding fluids (Plate 4).

3.2 Closed duct flow

Plates 5 to 8 show the phenomenon observed in the case of closed duct flow. Hydraulic condition is CASE 2 in Table 1. The black part is the tracer and the white arrow indicates the position of the organized structure of turbulence occurred. At the right hand side, the organized structure of turbulence occurred at either walls grows and moves to the center of duct (Plate 5). The both organized structure of turbulence interacts at the center and flow away (Plate 6 to 8). The organized structure of turbulence from the bottom is influenced by one from the upper wall in closed duct flow. On the other hand, the organized structure observed in

open channel flow is not reflected at the free surface and disperses along the free surface, because the free surface can propagate disturbance in a form of free surface waves.

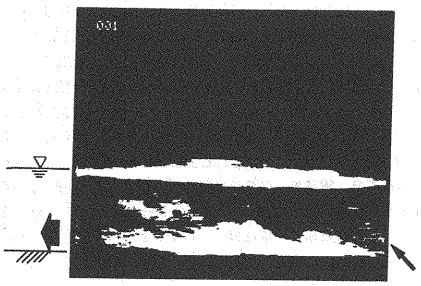

Plate 1

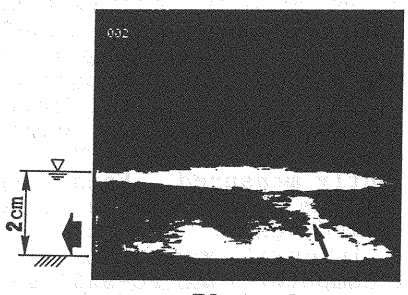

Plate 2

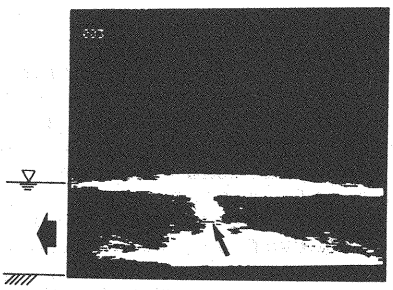

Plate 3

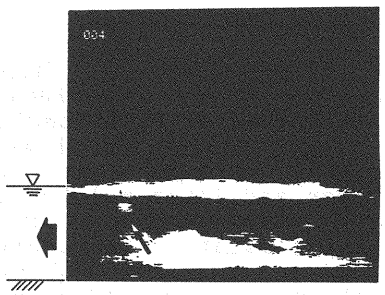

Plate 4

Plate 1~4 the organized structure of turbulence motions development in the open channel.(Re=5.3x10^4)

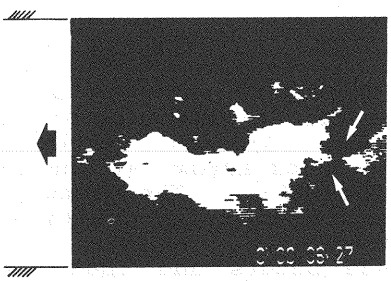

Plate 5

Plate 6

Plate 7

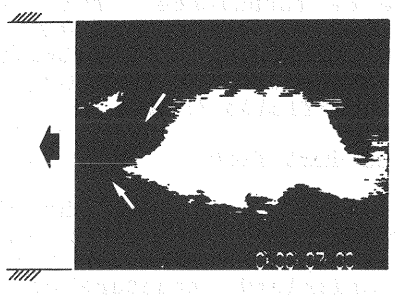

Plate 8

Plate 5~8 the organized structure of turbulence motions development in the closed duct.(Re=5.4x10^4)

4. MEAN VELOCITY AND TURBULENCE CHARACTERISTICS

4.1 Uniform flow

[1] Mean velocity

Figure 2 shows the mean velocity distribution of U versus y/ho(0<y/ho<1). The broken line indicates the log-law.

$$\frac{U}{U_*} = \frac{1}{\kappa}\cdot\ln\left(U_*\cdot\frac{y}{\nu}\right)+5.5, \quad \kappa=0.41$$

The solid line is log-wake law, applied at the outer region (y/h>0.15).

$$\frac{U}{U_*} = \frac{1}{\kappa}\cdot\ln y + A + \frac{2\Pi}{\kappa}\sin^2\left(\frac{\pi}{2}\cdot\frac{y}{h}\right)$$

where Π is Cole's coefficient, and Π=0.1,0.2,0.3 is drawn in Figure 2. In the case of open channel flow, the mean velocity distributes on the log-law in the all region from the bottom to the free surface. The maximum velocity point is located at y/ho=1.0, because the width of the channel is large enough (B/ho=13.0) to neglect the influence of the side wall. On the other hand, in the case of the closed duct, the distribution follows the log-law in the region of y/ho<0.8, the difference from the log-law becomes appreciable in the region y/ho>0.8 , and the velocity gradient approaches zero at the center line. It is found that the closed duct is controlled by the influence from both upper boundary and bottom, the flow structure in open channel flow is controlled only from the bottom.

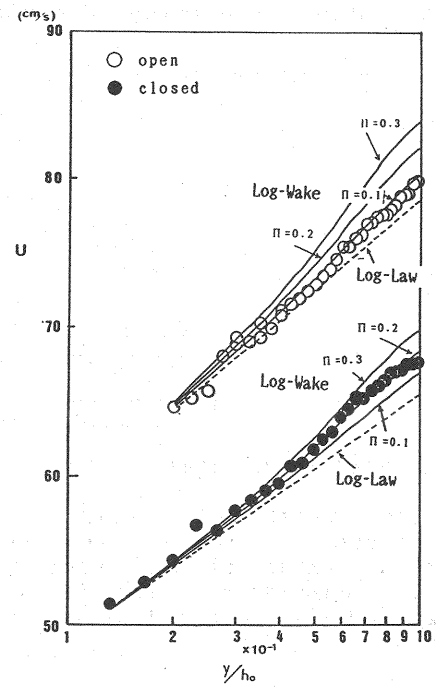

Figure 2 Velocity profile

[2] Turbulent stress

Figure 3 shows the turbulent stress profile ($\overline{uu}$,$\overline{vv}$). The vertical turbulent stress ($\overline{vv}$) distributes rather uniformly from y/ho=0.3 to y/ho=1 in either flow. The horizontal turbulent stress ($\overline{uu}$) decreases as y/ho increases from y/ho=0.2~0.3 to y/ho=1, and the value in open channel flow is larger than that in the closed duct. The distribution, is both uu and vv, of closed duct flow is roughly correspond with the result confirmed by some researcher. The distribution of the horizontal turbulent stress uu is conspicuously decreased, but one of the vertical turbulent stress vv is not declined larger than the horizontal turbulent stress uu.

[3] Numerical calculation

The applicability of k-ε was examined for open channel flow.

(1) Equations

The following three equations were solved by the finite difference method through the Crank-Nicholson scheme. The grid mesh was dy=0.1cm and dt=0.01sec. Eqs. 1, 2 and 3 were calculated as the initial value problem. The convergent result was solved as the steady solution.

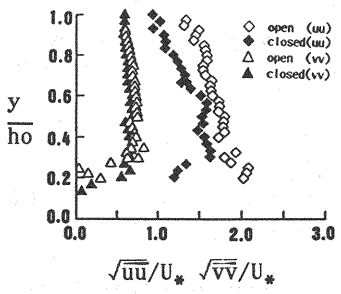

Figure 3 Turbulent stress

Table 2 shows the value of constants appeared in Eqs. 1, 2 and 3.

$$\frac{\partial U}{\partial t} = g\cdot\sin\theta + \frac{\partial}{\partial y}(\nu_t\frac{\partial U}{\partial y}) \qquad (1)$$

$$\frac{\partial k}{\partial t} = \nu_t(\frac{\partial U}{\partial y})^2 - \varepsilon + \frac{\partial}{\partial y}(\frac{\nu_t}{\sigma_k}\cdot\frac{\partial k}{\partial y}) \qquad (2)$$

$$\frac{\partial \varepsilon}{\partial t} = C_{\varepsilon_1}\cdot C_\mu\cdot k(\frac{\partial}{\partial^2 k})^2 - C_{\varepsilon_2}\frac{\varepsilon^2}{\partial y} + \frac{\partial}{\partial y}(\frac{\nu_t}{\sigma_\varepsilon}\cdot\frac{\partial \varepsilon}{\partial y}) \qquad (3)$$

Table 2 Constant Number

C_μ	C_{ε_1}	C_{ε_2}	σ_k	σ_ε
0.09	1.44	1.92	1.0	1.3

(2) Initial conditions

The first grid point is indicated by the subscript 's' in Eqs. 4 and 5 which is located at Y+=50 (Y+=YU*/ν). The measured value of the velocity distribution was used for the initial condition. The initial distribution of the turbulent energy and the energy dissipation rate were assumed uniform with the value shown by Eqs. 4 and 5.

$$\frac{k_s}{U_*} = \frac{1}{\sqrt{C\mu}} = 3.33 \qquad (4)$$

$$\varepsilon_s = \frac{U_*^3}{\kappa y_s} \qquad (5)$$

(3) Boundary condition

Firstly, the symmetrical condition at the center of the closed duct was examined. This condition was shown to Eq. 6, called a symmetric condition. It was applied to open channel flows. Secondly, an another boundary condition was applied. It was a simple model, called a free end condition at the cantilever, shown by Eq. 7.

$$\frac{\partial U}{\partial y} = \frac{\partial k}{\partial y} = \frac{\partial \varepsilon}{\partial y} = 0 \qquad (6)$$

$$\frac{\partial^2 U}{\partial y^2} = 0, \quad \frac{\partial k}{\partial y} = \frac{\partial \varepsilon}{\partial y} = 0 \qquad (7)$$

Figure 4 shows the comparison between the calculation and the measured values of the mean velocity distribution. The solid line is the calculation of the one dimensional k-ε model. In the case of closed duct flow using the symmetric condition, it distributes on the log-law from the bottom to the center. And it is satisfied with the symmetric condition. In open channel flows, it also distributes from the bottom to y/ho= around 0.8, but the calculation is different from measurements in the region of y/ho>0.8, and the symmetric boundary condition is inapplicable to the free surface. In other words, the free end condition is useful in open channel flow.

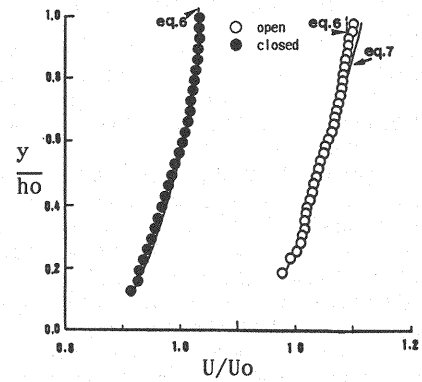

Figure 4 Velocity profile

[4] Turbulent energy

Figure 5 shows the distribution of the turbulent energy k/U_*^2 which is evaluated by $k=1.5\cdot(u^2+v^2)/2$, because of lack of the span wise turbulence w. The symmetric boundary condition gives good agreement, the measurement in closed duct flow. On the other hand, the free end condition gives better results than the symmetric condition. However it should be noted that the measurement shows the smaller value near the free surface which phenomena fact can not be included in the model.

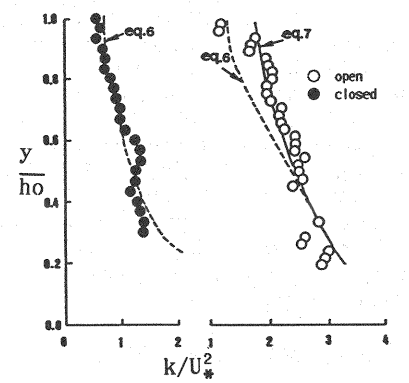

Figure 5 Kinematic energy

[5] Dissipation ratio

Figure 6 shows the distribution of the turbulent dissipation ratio $\varepsilon\cdot ho/U_*^3$. Using the symmetrical condition gives good agreement with the measurement in the duct flow, but the agreement is not so good in the case of open channel flow. In the case of the free end condition, a good agreement is obtained. But the measurement reduces near the free surface, and the free end condition is not able to displayed this tendency in the same case of the turbulent energy.

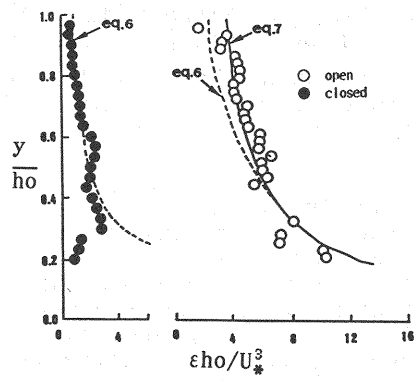

Figure 6 Dissipation ratio

4.2 Wake flow

In the case of setting the vertical cylinder in the uniform flow, the standing waves are remarkably generated in the wake of open channel

flow. It is expected that the turbulent structure of the open channel flow is considerably different from one of the closed duct flow.

Horizontal turbulent stress

Figure 7 shows some example of measurements of the horizontal turbulent stress profile. The hydraulic condition CASE 3 and CASE 4 in Table 1. The vertical cylinder(Φ=3.2cm) is placed up 45cm from the measuring point at center of the flume. In the case of closed duct flow, it reduces toward the center line in the uniform flow. It is recognized characteristics of wake that it distributes uniform from y/ho=0 to y/ho=1 in the wake flow. On the other hand, in the case of open channel flow, the horizontal turbulent stress decreases toward the free surface in the uniform flow. In the case of wake flow, its distribution for x=20cm is about constant from the wall to the free surface, and for x=50cm distributes uniformly near the free surface and its distribution decreases with the increase of y/ho in the region of y/ho<0.5. The wake in the open channel is faster to decay than one in the duct, and so that the structure of the wall turbulence quickly recovers in the case of open channel flow.

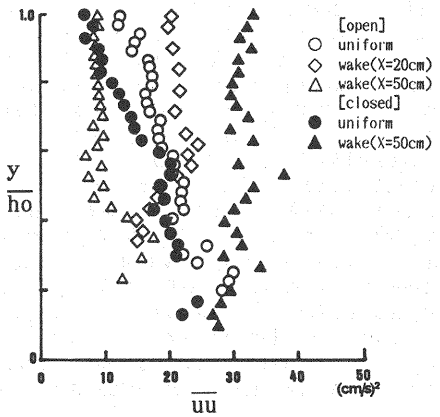

Figure 7 Turbulent stress ($\overline{uu}$)

Vertical turbulent stress

Figure 8 shows the vertical turbulent stress profile. In the case of the uniform flow and of the wake flow except the duct, it distributes uniformly. In the case of the duct in the wake flow, it increases toward the center of the duct.

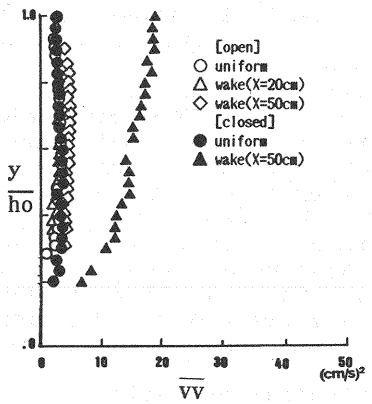

Figure 8 Turbulent stress ($\overline{vv}$)

5. CONCLUSION

It is found that the following difference at the mean velocity and the turbulent stress distribution between open channel flow and closed duct flow.

(1)In the mean velocity distribution, the conventional symmetrical boundary condition in closed duct flow is inapplicable at the free surface in open channel flow.

(2)The free surface restricts the turbulent energy.

(3)The wake in the open channel is faster to decay than in the duct, and the structure of the wall turbulence, in open channel flow, recovers quickly.

(4)The large scale motion of turbulence from the either boundaries is interacted each other at the center of the duct. The turbulent structure of open channel flow, on the other hand, is different from

one of closed duct flow, because the large scale motion of turbulence from the bottom is not reflected at the free surface.

ACKNOWLEDGMENT

The authors wish to express the gratitude to the technical official Mr. E.SATO for much helpful advice, and also to Mr. Y.KURIYAMA for his assistance in making measurements.

The publication of the present paper is financially supported by the Ogawa Commemoration Fund.

REFERENCES

1. Nezu, I. and H. Nakagawa : Numerical calculation of turbulent open-channel flows in free-surface effects -- computer simulation by a modified k-ε Turbulence model --, Annuals, Disas.Prev.Inst., Kyoto Univ., No29b-2, 1986.
2. Laufer, J. : The structure of turbulence in fully developed pipe flow, NACA Tech. Rep. No.1174, 1955.
3. Hussain, A.K.M.F. and Reynolds, W.C. : Measurements in fully developed turbulent channel flow, pp.568-580, Trans. of ASME, 1975.

APPENDIX - NOTATION

The following symbols are used in this paper:

ho	= Depth of flow;
k	= Turbulent energy;
suffix s	= First point grid;
u, v, w	= Turbulent intensity in the x, y and z direction respectively;
x, y, z	= Streamwise, vertical and spanwise direction, respectively;
$Fr=\frac{Uo}{\sqrt{gho}}$	= Froude number;
R	= Hydraulic Radius;
$Re=\frac{Uoho}{\nu}$	= Reynolds number;
U	= Local mean velocity in the x direction;
Umax	= Maximum mean velocity;
Uo	= Mean bulk velocity;
U_*	= Friction velocity;
ε	= Dissipation rate of turbulence;
κ	= Von Karman's constant;
ν	= Kinematic viscosity of water; and
ν_t	= Kinematic eddy viscosity.

(Received June 7, 1990; revised September 10, 1991)